Oscillatory MEG gamma band activity dissociates perceptual and conceptual aspects of visual object processing: A combined repetition/conceptual priming study

Uwe Friese [a,*,1], Gernot G. Supp [b,1], Joerg F. Hipp [b,c], Andreas K. Engel [b], Thomas Gruber [a]

[a] Institute of Psychology, University of Osnabrueck, Germany
[b] Department of Neurophysiology and Pathophysiology, University Medical Center Hamburg-Eppendorf, Hamburg, Germany
[c] Centre for Integrative Neuroscience, University of Tübingen, Germany

A B S T R A C T

We used a combined repetition/conceptual priming task to investigate attenuations of induced gamma-band activity (iGBA) due to prior experience. We hypothesized that distinguishable iGBA suppression effects can be related to the processing of (a) perceptual aspects, and (b) conceptual aspects of cortical object representations. Participants were asked to perform a semantic classification task with pictures of real world objects and their semantically corresponding words, using a design that isolated distinct levels of the neural suppression effect. By means of volumetric source analysis we located stimulus domain-specific iGBA repetition suppression effects (60–90 Hz) in temporal, parietal, and occipital areas of the human cortex. In contrast, domain-unspecific iGBA repetition suppression, corresponding to conceptual priming, was restricted to left temporal brain regions. We propose that the selective involvement of left temporal areas points to the activation of conceptual representations, whereas more posterior temporal, parietal, and occipital areas probably reflect perceptual aspects of higher-order visual object processing.

© 2011 Elsevier Inc. All rights reserved.

Introduction

The repeated processing of stimuli commonly leads to faster and more accurate responses in a variety of tasks (repetition priming), even if the repetition itself is task-irrelevant. With respect to the underlying brain mechanisms, neuroimaging studies using positron emission tomography (PET) and functional magnetic resonance imaging (fMRI) have associated repetition priming predominantly with decreased brain activity following stimulus processing. Consequently, this phenomenon has been termed repetition suppression (for reviews see Henson, 2003; Grill-Spector et al., 2006; Schacter et al., 2007). According to Desimone (1996) repetition suppression might represent a by-product of the "sharpening" of stimulus representations in the cortex. In this view, objects can be cortically processed by sparser neuronal assemblies following repeated occurrences of a given stimulus which in turn leads to decreased activation as seen in studies using PET and fMRI (Wiggs and Martin, 1998). Further empirical evidence supporting the sharpening hypothesis originates from electrophysiological studies using electro-encephalography (EEG) and magnetoencephalography (MEG). Even though repetition-dependent changes are already evident in the amplitude reduction of the averaged scalp-recorded potentials, i.e. ERPs (e.g., Race et al. 2010; Voss et al., 2010), the analysis of oscillatory

brain activity in the gamma-band frequency range (>30 Hz) seems to be particularly suited to unravel the nature of cortical object processing in greater detail.

Resting on a broad scope of electrophysiological evidence, including data from animal and human patient studies using intracranially implanted electrodes, transient induced gamma band activity (iGBA) is assumed to reflect the synchronized oscillatory activity of distributed neuronal populations engaged in the representation of objects (Tallon-Baudry and Bertrand, 1999; Varela et al., 2001; Engel et al., 2001; Jensen et al., 2007). Several studies have shown that scalp-recorded power and phase synchronization of iGBA decreases for repeatedly presented pictures of objects or words (Gruber and Müller, 2002; Gruber and Müller, 2005; Fiebach et al., 2005; Conrad et al., 2007), but the precise origins of these attenuation effects are still unknown. In particular, it is unclear to what extent iGBA mirrors perceptual and/or conceptual aspects of visual object processing. Most studies employed repetition priming paradigms such that physically identical stimuli were presented as prime and target stimuli. It is therefore not possible to conclude whether iGBA attenuation on repeated occurrences of the same stimulus results only from facilitated processing of perceptual stimulus features, or if conceptual processing also plays a role. Some evidence that gamma band activity is not merely reflecting low-level perceptual features comes from studies on crossmodal sensory processing (Schneider et al., 2008; Schneider et al., 2011). For instance, studying the integration of visual and auditory information Schneider et al. (2008) presented pictures of objects followed by congruent or incongruent

---

* Corresponding author at: University of Osnabrück, Institute of Psychology, Seminarstr. 20, D-49074 Osnabrück, Germany. Fax: +49 541 969 4922.
E-mail address: uwe.friese@uni-osnabrueck.de (U. Friese).
[1] These authors contributed equally.

environmental targets sounds (e.g., the picture of a sheep and the sound produced by sheep or by a bell). Induced GBA was reported to be larger if the bimodal information was congruent, suggesting that gamma band oscillations are related to the formation of multisensory conceptual representations. Further indications for an involvement of gamma band oscillations at higher processing levels come from a word repetition priming experiment using words and word homophones (Matsumoto and Iidaka, 2008). An iGBA suppression effect was found if a prime word (e.g., "pair") was followed by a homophone target word (e.g., "pear"), indicating a role of gamma band oscillations at the phonological level above the orthographical representation.

Recently, a compelling study showed that scalp-recorded EEG signals can be contaminated with ocular artifacts (miniature eye movements) that in particular might impact the interpretation of iGBA (Yuval-Greenberg et al., 2008). In detail, the authors presented evidence that iGBA, commonly found in scalp-recorded EEG approximately 200–300 ms following stimulus onset, is time-locked to – and therefore incorporates – the so called saccadic spike potential. Up to now, different algorithms have been proposed to detect and remove saccadic spike potentials from the EEG (Keren et al., 2010; Hassler et al., 2011), but the validity of these methods has yet to be established. In our study we recorded MEG which represents a reference-free recording technique and therefore should not be susceptible to the broad and distant spatial transmission of frontal eye movement artifacts due to referencing (see Discussion). In addition, we analyzed iGBA in source space, and none of the signals' sources in the gamma frequency band was located at frontal brain sites or around the orbital cavities of the eyes. Furthermore, we investigated two time windows, i.e. 200–400 ms and 400–700 ms after stimulus onset. The 400–700 ms time interval is set notably later than the reported critical microsaccadic iGBA effects, and it is located within the ongoing iGBA that can often be observed until the offset of a stimulus (Gruber and Müller, 2002; Fries et al., 2008; Haenschel et al., 2009; Hassler et al., 2011).

In the current study, we employed a combined repetition and conceptual priming paradigm to dissociate iGBA sharpening effects directly between perceptual and conceptual levels. The stimuli consisted of pictures of real world objects and their semantically matched words, so that within a given prime-target stimulus-pair a word could be used as a semantic prime for a subsequent picture (target) and vice versa. In the present experiment, participants were instructed to classify each stimulus, i.e. pictures or their semantically matched words to be either "natural" or "man-made". Stimuli were repeated either in the same domain as during the initial presentation (picture–picture or word–word) or in a different domain (picture–word or word–picture). Our main objective was to demonstrate repetition-dependent iGBA attenuation during visual object processing in response to prime-target stimulus pairs which were identical at the conceptual level but different at the perceptual level. This supposition follows directly from the sharpening approach but – to the best of our knowledge – has not been addressed yet. More precisely, we expected to identify iGBA reductions after repeating the same physical stimulus (e.g., picture follows picture), as well as after repeating the semantic information by using a cross-domain switch in stimulus presentation (picture follows semantically corresponding word). Inferring from priming studies with fMRI acquisitions, we assumed that within-domain suppression effects should reside in cortical areas associated mostly with perceptual processing (Wagner et al., 2000; Henson and Rugg, 2003). In contrast, cross-domain suppression effects should be restricted primarily to areas involved in conceptual processing. Schacter et al. (2007) proposed that, for visual stimuli, perceptual cortices show a gradient of stimulus specificity with greater specificity occurring in posterior regions compared to more anterior sites. Importantly, regions of the lateral temporal cortex were reported to respond to conceptual components of repetition priming across different stimulus domains. Therefore, if prior experience-dependent iGBA reductions reflect perceptual as well as conceptual aspects of priming, we expect that these distinct levels of visual object processing are associated with neural suppression in dissociable regions of mainly temporal, parietal, and occipital cortex. Specifically, we hypothesized that conceptual priming, i.e. cross-domain iGBA repetition suppression, would be associated with temporal cortex areas. To this end, we combined Morlet wavelet analysis of oscillatory brain activity (Bertrand and Pantev, 1994) with a volumetric source localization approach (Variable Resolution Electromagnetic Tomography, VARETA; Bosch-Bayard et al., 2001) to characterize the underlying brain sources of gamma band activity.

Methods

Participants

A total of 22 healthy university students (11 females, on average 26.3 years old, SD = 3.7) received monetary compensation for participation. None of the participants reported a history of neurological or psychiatric disorders. All participants had normal or corrected-to-normal vision. Informed consent was obtained from all participants according to the Declaration of Helsinki.

Design

The design of the experiment was guided by two factors: conditions and stimulus domain (pictures versus words). Levels of conditions correspond to: (1) *first* object presentations, (2) object repetitions in the *same* stimulus domain, and (3) object repetitions in the *different* stimulus domain. Hence, the following six combinations were used for analysis:

– Pictures-first: initial picture object presentation (prime stimuli)
– Pictures-same: repetition of a picture object after a picture prime
– Pictures-different: repetition of a picture object after a word prime
– Words-first: initial word object presentation
– Words-same: repetition of a word object after a word prime
– Words-different: repetition of a word object after a picture prime.

Stimuli and procedure

See Fig. 1 for exemplary stimuli and a schematic outline of the presentation sequence. Pictures with line-drawings of 320 objects (taken from Snodgrass and Vanderwart, 1980; Alario and Ferrand, 1999) and the 320 words denoting the corresponding objects served as stimuli. In total, there were four combinations of prime-target stimulus pairings depending on the presentation domain (picture versus word) and the presentation position (first versus repeated presentation): picture–picture, word–word, picture–word, and word–picture, resulting in 80 stimuli presented in each of the four combinations. Objects were assigned randomly, and no object was presented in more than one prime-target combination for each participant. Additional 80 pictures and 80 words were presented only once as filler items to decrease expectancy effects concerning the second presentation of a given object. Thus, a total of 800 stimuli were presented in pseudo-random order during the experiment. Prime and target stimuli were separated by at least two and not more than three intervening objects. Participants were instructed to decide for each stimulus whether the referred objects were either man-made or of natural origin. In order to allow accommodation to the task, before the start of the experiment each participant performed 20 practice trials consisting of stimuli not used in the main experiment. Participants responded by pressing buttons of a response box using their left or right index finger. The response-to-button assignment was counter-balanced across participants. A calibrated LCD projector outside the magnetically shielded room projected the stimuli covering
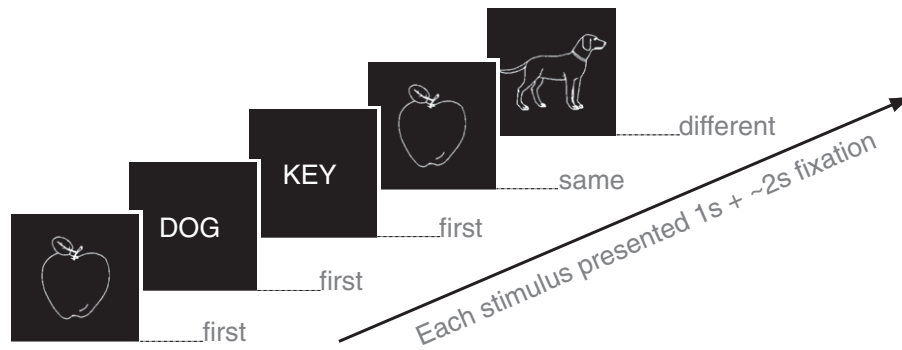
Fig. 1. Stimulus sequence example. Objects are presented twice as pictures or words. Subsequent to the first presentation of an object, repetitions occur within the same stimulus domain (*apple*) or in the different stimulus domain (*dog*). In this example only pictorial repeated objects are shown but word stimuli were repeated analogously.

approximately 6×6° visual angle onto a back projection screen in front of the participant's head. The presentation sequence started with a fixation cross presented in the center of the screen (500 ms plus up to 300 ms jitter). Subsequently, the object was presented for 1000 ms. This was followed by the fixation cross for 500 ms and an "X"-character for 900 ms, indicating the preferred time for eye blinks. One trial lasted between 3000 and 3300 ms. Short breaks intermitted the experiment after blocks of 100 trials.

MEG recordings

Electromagnetic activity was recorded using a 275-channel whole-head MEG system (VSM, CTF Systems Inc.) in a magnetically shielded room, low-pass filtered online (cutoff frequency: 300 Hz), and sampled at 1200 Hz. Trials containing eye blinks, saccades, muscle artifacts, and signal jumps were rejected from further analysis using semiautomatic procedures implemented in the Fieldtrip software package (http://www.ru.nl/fcdonders/fieldtrip/). Data were resampled at 400 Hz, and submitted to spectral analysis as described below.

Data analysis: behavioral data

Participants' averaged accuracy data and mean reaction times of correct responses between 200 ms and 1000 ms were subjected to 3 (condition: first, same, different)×2 (domain: pictures, words) analyses of variance (ANOVAs). Priming effects were computed by subtracting first minus same and first minus different separately for picture and word targets. We illustrate priming effects graphically using 95% confidence intervals following recommendations by Loftus and Masson (1994). Reliable differences–corresponding to the results of one-sample t-tests–can be assumed if the 95% confidence bounds do not include zero.

Data analysis: induced spectral changes

We used Morlet wavelet analysis to investigate spectral changes of oscillatory activity (Bertrand and Pantev, 1994). The general methodology has been described in several publications (e.g., Tallon-Baudry et al., 1997; Tallon-Baudry and Bertrand, 1999; Gruber and Müller, 2006) and will only be summarized here. Prior to wavelet analysis, we subtracted the average signal from the data. Morlet wavelets were specified with a width of 7 cycles per wavelet for a frequency range of 2 to 148 Hz. For each trial, Morlet wavelet analysis results in time-frequency (TF) representations of the signal amplitude in specified frequency bands. Since iGBA occurs with a jitter in latency from trial to trial, it tends to cancel out in the averaged evoked potential. Averaging TF energy across single-trials allows to study non-phase-locked activity, i.e. *induced* responses.

Our focus in this study was on modulations within induced activity in the gamma band but we also analyzed lower frequencies.[2] To identify the latency and frequency ranges of induced activity in the gamma, alpha, and theta range, we generated TF plots of mean baseline-corrected spectral power averaged across all initial stimulus presentations (primes) and across regional means. Power estimates after stimulus onset were divided by average power estimated from the baseline (200–0 ms before stimulus onset). For the gamma frequency range we chose parietal and occipital sensors, for the alpha and theta range we averaged across all sensors. Further analyses of induce gamma band activity were carried out for frequencies between 60 and 90 Hz in two time windows, i.e. 200–400 ms and 400–700 ms after stimulus onset. This choice was based on the following reasons. The first window 200–400 ms was chosen because the majority of previous studies have reported transient effects associated with the iGBA peak response within this time range (e.g., Gruber and Müller, 2005). On the other hand, ongoing iGBA effects following the maximal amplitudes have also been suggested (Fries et al., 2008; Hassler et al., 2011). Hence, based on visual inspection of the TF-plot we selected 400–700 ms to study ongoing responses. Moreover, we defined the frequencies and time windows for alpha (10 Hz; 300–900 ms), and theta band activity (6 Hz; 300–900 ms) based on visual inspection of the respective TF-plots.

In a first analysis step, we averaged induced power estimates within sensor clusters and subjected these data to cluster×time×domain×condition ANOVAs. For effects including the factor cluster, we adjusted the degrees of freedom according to the Greenhouse–Geisser method. Results associated with $p<.05$ are considered to be significant, and we additionally report effects with $p<.1$ on an exploratory basis. In case of significant main effects of condition or interaction effects including the factor condition, we based further evaluations on difference scores analogous to priming effects, i.e. first presentations minus repetitions in the same domain, and first presentations minus repetitions in the different domain. Thus, positive difference scores denote repetition suppression, and negative differences indicate repetition enhancement. As with priming effects, we graphically illustrate these differences using error bars with 95% confidence intervals (Fig. 4).

Data analysis: source localization

To localize the generators of oscillatory MEG activity we used a 3D grid of points (or voxels) that represent possible sources of the signal. A total of 3244 grid points (7.00 mm grid spacing) and the recording array were placed in registration with the ICBM-152 average brain template produced by the Montreal Neurological

---

[2] We also analyzed evoked activity in gamma, alpha, and theta bands but since we did not find any significant repetition-dependent modulations these analyses are not presented here.

Table 1
Average response times (RT) and accuracies.

	Pictures			Words		
	First	Same	Different	First	Same	Different
Mean RT in ms (SD)	653 (83)	600 (66)	642 (74)	743 (101)	659 (93)	689 (86)
Mean accuracy (SD)	.93 (.04)	.94 (.03)	.94 (.03)	.90 (.05)	.94 (.04)	.92 (.04)

Note. Means and standard deviations (SD) of responses to initial stimulus presentations (first) and repetitions in the identical stimulus domain (same) and with a domain switch (different).

Institute. Subsequently, single-trial VARETA analyses were used for source reconstructions (for a detailed description see Bosch-Bayard et al., 2001; Gruber et al., 2006b). This method is based on a discrete spline distributed inverse model and reveals estimates of the primary current densities (PCDs) in source space which are the spatially smoothest solutions compatible with the observed scalp topographies. To characterize the generators of induced gamma activity during picture and word processing in the two time windows, we first subjected the PCD estimates of each participant to four voxel-by-voxel 1-way ANOVAs across conditions (first vs. same vs. different) separately for both time windows and stimulus domains. The resulting statistical parametric maps (SPMs) were thresholded corresponding to a false discovery rate of $q = .01$ (Genovese et al., 2002) and illustrated as overlays on an MRI brain template (Fig. 5). The coordinates of the maximum amplitude voxels within each significant cluster were taken as centers to define spherical regions of interest (ROIs) with 10 mm radius (see Table 3 and Figs. 5 and 6). Averages across voxels within each ROI were further explored analogous to the statistical analyses in sensor space.

Data analysis: phase-locking

We computed phase-locking values (PLVs) according to the method proposed by Lachaux et al. (1999). This allows to examine phase synchrony independent of signal amplitudes. Since phase-locking analysis at the scalp surface can be compromised by neural sources eliciting activity at distant sensor sites through volume conduction, we reconstructed the MEG signals at each sensor for all conditions based on a subset of the regions of interest identified in the previous analysis step (for a detailed description of this approach, see Gruber et al., 2006a). We limited the analysis of PLVs to sensors which were most sensitive to the sources involved in the generation of the iGBA 400–700 ms. For this purpose, separate forward solutions were

Table 2
Sensor space iGBA ANOVA results.

Effect	df (Greenhouse–Geisser corrected)	F	p	$\eta^2_{partial}$
TF-window	1, 20	2.2	.15	.1
Cluster	1.4, 27.8	36.6	<.01	.65
Domain	1, 20	61.0	<.01	.75
Condition	2, 40	10.3	<.01	.34
Window × cluster	2.4, 48.2	20.2	<.01	.50
Window × domain	1, 20	7.3	.01	.27
Cluster × domain	2.4, 48.3	40.4	<.01	.67
Window × cluster × domain	3.6, 71.4	2.3	.07	.10
Window × condition	2, 40	5.0	.01	.20
Cluster × condition	8.2, 164.5	3.5	<.01	.15
Window × cluster × condition	8.3, 167.1	1.5	.17	.07
Domain × condition	2, 40	1.2	.30	.06
Window × domain × condition	2, 40	2.2	.13	.10
Cluster × domain × condition	8.4, 168.8	0.6	.82	.03
Window × cluster × domain × condition	9.6, 192.5	2.1	.03	.10

Table 3
Anatomical descriptions and MNI coordinates of the centers of gravity of iGBA sources.

ANOVA	Anatomical description	L/R	X,Y,Z (MNI coordinates)
200–400 ms			
Pictures	Posterior cingulate cortex (ROI 1)	RH	14, −40, 41
Words	Anterior superior temporal gyrus (ROI 2)	LH	−57, 3, 5
400–700 ms			
Pictures	Temporal–parietal–occipital junction, TPO (ROI 3)	LH	−43, −69, 12
	Cuneus, precuneus (ROI 4)	LH	−2, −69, 12
	Cuneus, precuneus	RH	7, −62, 12
	Posterior superior temporal gyrus (ROI 5)	LH	−43, −33, 5
	Anterior middle temporal gyrus (ROI 6)	LH	−70, −11, −17
Words	Middle occipital gyrus[a]	LH	−36, −69, 19

Abbreviations: LH: left hemisphere, RH: right hemisphere.
[a] This cluster falls within ROI 3.

estimated for each ROI and condition, and we selected the 30 sensors (5 ROIs × 6 conditions) for which the reconstructed MEG signal was maximal. Since for some conditions the same sensors were found to be most sensitive, this procedure resulted in a total of 12 selected sensors for picture conditions and 11 sensors for word conditions. Subsequently, conventional phase-locking analysis for the selected sensors was conducted. For each condition, significant PLVs were determined with one-sample t-tests ($p < .01$) and illustrated as solid lines connecting the respective sensors on topographical maps. The topographical maps were created by averaging the forward solutions for picture conditions and word conditions respectively. χ^2-tests were used to evaluate if the number of significant PLVs differed between initial object presentations and repeated object presentations (first vs. same vs. different).

Results

Response times and response accuracy

Average response times (RT) and response accuracy rates are depicted in Table 1. A within-subjects 3 (condition) × 2 (domain) ANOVA for RTs revealed significant main effects of condition ($F_{2,40} = 69.6$, $p < .01$) and domain ($F_{1,40} = 100.5$, $p < .01$) as well as a significant interaction effect ($F_{2,40} = 13.8$, $p < .01$). For response accuracy rates, the main effects of condition ($F_{2,40} = 3.6$, $p = .04$) and domain ($F_{1,40} = 4.7$, $p = .04$) were significant but the interaction effect was not ($F_{2,40} = 1.4$, $p = .27$). Priming effects are illustrated in Fig. 2. For response times, all priming effects were reliable, i.e., no lower confidence bound was smaller than zero. Accuracy rates were generally high, and a reliable priming effect occurred for word objects following word primes (words-same).

Induced oscillatory activity

Fig. 3A shows baseline-corrected time by frequency (TF) plots for induced oscillatory activity averaged across initial picture and word presentations (see Methods section for details). The spectrum in the induced gamma range showed maximal increase between approximately 180–750 ms and 60–100 Hz. TF plots for induced spectral amplitudes in the lower frequency bands revealed a dissociation between alpha and theta band activity, i.e. alpha power decreased most strongly from 300 to 900 ms, while theta power increased during the same interval.

The topographies of averaged data corresponding to the selected TF window are depicted as grand mean spherical spline interpolated amplitude maps separately for picture and word stimuli (Fig. 3B). Increased iGBA was distributed primarily over occipital and parietal
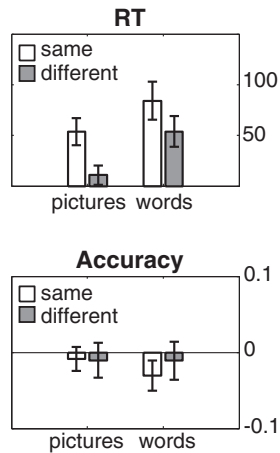
Fig. 2. Behavioral priming effects. Differences of mean response time (RT) in milliseconds and mean response accuracy rates between first presentations and repetitions in the identical stimulus domain (same) and with a domain switch (different). Error bars indicate 95% confidence intervals.

cortex areas. The induced alpha band activity reduction occurred over posterior cortex sites, and induced theta activity was pronounced at central and frontal sensors. Next, for each participant, time window, condition, and stimulus domain, we averaged the data in ten sensor clusters (left and right hemisphere frontal, central, temporal, parietal, and occipital sensor sites). Since the results were highly similar, and for improved clarity, we further reduced the number of clusters for iGBA to a total of five clusters: bilateral frontal, bilateral central, left temporal, right temporal, and bilateral occipital sites (see illustration in the middle column of Fig. 4).

Induced gamma band activity

Averaged data were subjected to a cluster × time window × domain × condition ANOVA in which all factors were found to modulate iGBA significantly. See Table 2 for a detailed listing of effects. Most importantly, the three way interactions cluster × time × condition and type × time × condition indicate complex differential influence of these factors. To further illustrate these iGBA effects in sensor space we built difference scores analogous to priming effects (first minus repeated object presentations) and plotted these as indicators of repetition suppression effects within the five clusters separately for both stimulus domains and in both time windows (Fig. 4). The left column of Fig. 4 shows that picture repetition suppression effects were only found in the *same* condition 400–700 ms after stimulus onset (gray bars) at central, left temporal, and occipital sensors. For words, repetition suppression was evident in the *same* condition 200–400 ms at left temporal sensors, as well as in the *same* condition 400–700 ms at occipital sensors.

Induced low-frequency activity

For induced alpha band activity, a cluster × domain × condition ANOVA led to significant effects of cluster ($F_{2.5,44.8} = 35.9$, $p < .01$) as well as significant interactions cluster × domain ($F_{3.9,77.2} = 2.6$, $p = .04$) and cluster × condition ($F_{4.7,28.2} = 2.3$, $p = .03$). Collapsing data across domain, we explored the cluster × condition interaction by testing repetition suppression effects within each cluster. This analysis revealed that alpha band activity decrease (with respect to baseline) in left temporal regions was attenuated when stimuli were repeated in the same domain ($t_{20} = -3.2$, $p < .01$). Additionally, also for the same-condition, there was a marginally significant increase in alpha band suppression at right parietal sensors ($t_{20} = 2.1$, $p = .05$). For theta band activity, only the effects of cluster ($F_{3.9,77.4} = 21.0$, $p < .01$) and cluster × domain ($F_{5.6,111.3} = 3.4$, $p < .01$) were significant. Given our
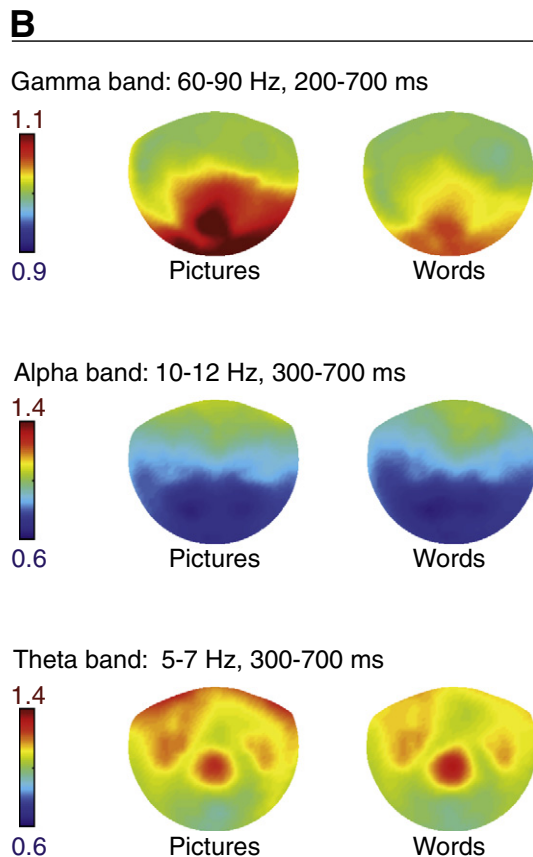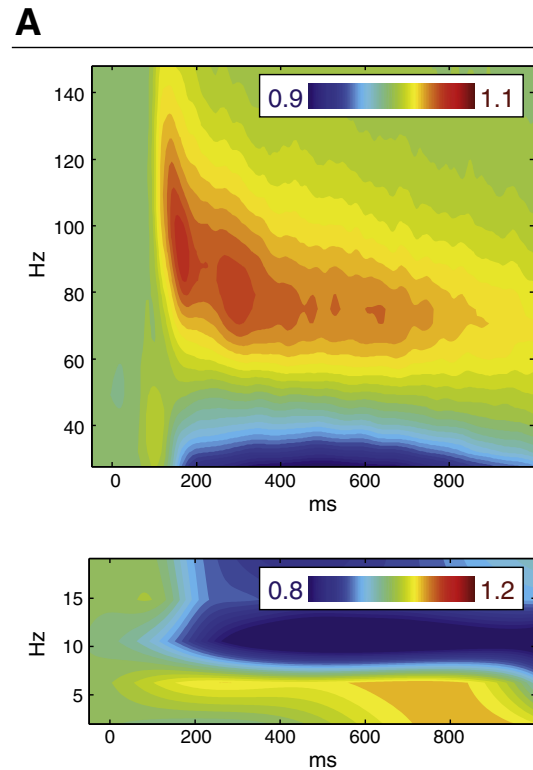
Fig. 3. Induced oscillatory activity. Panel A depicts time by frequency plots of induced oscillatory activity separately for the gamma range (approx. 40–140 Hz) and for lower frequency bands (approx. 5–15 Hz). In panel B, grand mean spherical spline interpolated amplitude maps for induced responses to picture and word stimuli are shown for selected time-frequency windows in the gamma, alpha, and theta range. Amplitudes are expressed as signal changes relative to the baseline period.
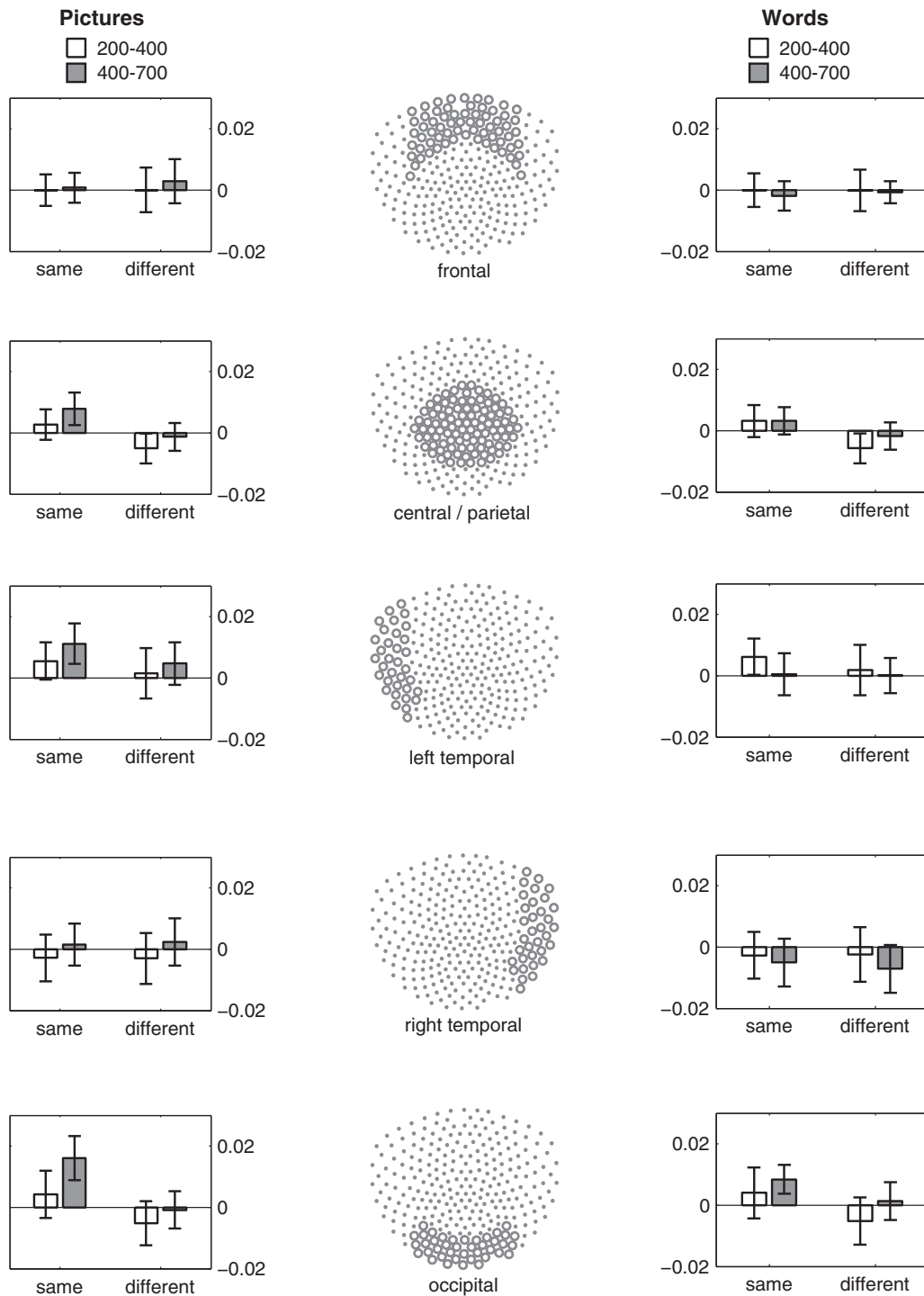
Fig. 4. Induced GBA repetition effects in sensor space. In the middle column, schematic representations of five sensor clusters are shown. Within these clusters, we averaged iGBA amplitude changes with respect to baseline for picture and word stimuli in two time windows (200–400 ms and 400–700 ms). Bars represent grand mean repetition effects analogous to priming effects. Difference scores were built between first presentations and repetitions of an object in the identical stimulus domain (same) as well as between first presentations and repetitions of an object in the other stimulus domain (different). Positive bars indicate repetition suppression. Error bounds indicate 95% confidence intervals. Asterisks (*) indicate significant priming.

primary interest in induced gamma band oscillations and repetition dependent modulations we did not further explore these effects.

Source localization

To investigate the cortical sources of significant sensor space iGBA repetition suppression effects, VARETA source localization analyses were conducted. Fig. 5 illustrates statistical parametric maps (SPM)

corresponding to the results of ANOVAs across conditions for pictures and words in the two time windows (see Table 2 for additional information). In the 200–400 ms range, picture conditions were associated with modulated iGBA in the right posterior cingulate gyrus (ROI 1), whereas word conditions showed differential source activity in the left anterior superior temporal gyrus (ROI 2). From 400 to 700 ms, a network of left temporal and bilateral occipital and parietal regions were modulated by picture conditions (ROI 3–6). The cluster
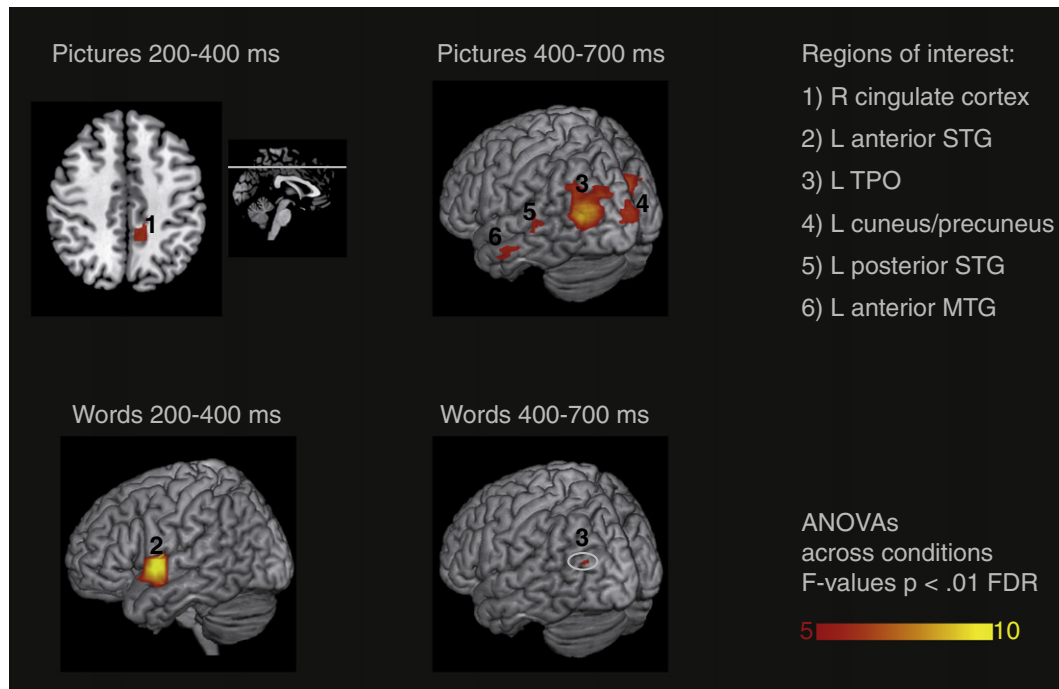
Fig. 5. Sources of induced gamma band activity. Statistical parametric maps corresponding to the results of ANOVAs across conditions (first vs. same vs. different) separately for both stimulus domains (pictures in upper panels vs. words in lower panels) and two time windows (200–400 ms on the left vs. 400–700 ms on the right). Significant regions are projected onto an MRI brain template using MRIcron software (http://www.cabiatl.com/mricro/mricron/). Numbers adjacent to significant clusters denote the assigned region of interest used for further analyses. Abbreviations: L—left hemisphere, R—right hemisphere, MTG—middle temporal gyrus, STG—superior temporal gyrus, TPO—temporal–parietal–occipital junction area.

defining ROI 3 is located at the junction of temporal, parietal, and occipital cortex (TPO). ROI 4 comprises large medial regions in cuneus and precuneus (not fully visible in Fig. 5). Right hemisphere homologue areas of ROI 4 have also been found but are not included as a separate ROI because we do not expect hemispheric differences in these regions. ROI 5 and ROI 6 are located in left superior and middle temporal gyrus respectively. A small cluster at the junction of the left middle temporal gyrus and the middle occipital gyrus was also found significant for word conditions (overlapping with ROI 3). Analogous to the analysis in sensor space, we derived difference scores from the regions of interest to directly investigate repetition suppression for same versus different modality stimulus repetitions.

For pictures, a ROI × time × conditions ANOVA resulted in a marginally significant effects of ROI ($F_{2.8,60} = 2.6, p = .06, \eta^2_{\text{partial}} = .12$) and time ($F_{1,20} = 4.2, p = .05, \eta^2_{\text{partial}} = .17$) as well as a significant ROI × conditions interaction ($F_{3.4,68} = 3.1, p = .03, \eta^2_{\text{partial}} = .13$). No significant effects in the same ANOVA model were found for words (all p-values > .1). Repetition suppression in source space is further illustrated in Fig. 6. As can be seen in the left column of Fig. 6, for pictures, no significant repetition suppression occurred in the 200–400 ms time window (error bounds of all white bars include zero). Repetition suppression selective to the pictures-same condition was found in the posterior cingulate gyrus (ROI 1), in the TPO region (ROI 3) and in cuneus/precuneus (ROI 4). In the left posterior STG (ROI 5) and anterior MTG (ROI 6), repetition suppression was not restricted to same domain primes but occurred for both, pictures-same and pictures-different. Next, we wanted to explore if the apparent dissociation between prime domain independent repetition suppression in left temporal areas versus prime domain specific attenuation effects in more posterior occipital areas was reliable. For this purpose, we averaged data in temporal regions (ROI 5 and 6) and more posterior TPO and occipital regions (ROI 3 and 4) and tested for an interaction between region (temporal vs. occipital) × condition (same vs. different). The corresponding ANOVA revealed only marginal

main effects of region ($F_{1,20} = 3.8, p = .07, \eta^2_{\text{partial}} = .16$) and condition ($F_{1,20} = 3.8, p = .07, \eta^2_{\text{partial}} = .16$) but a significant interaction effect ($F_{1,20} = 5.8, p = .03, \eta^2_{\text{partial}} = .23$).

For words, the right column of Fig. 6 depicts that the only significant repetition suppression effects were evident in the left STG (ROI 2) for both words-same and words-different conditions from 200 to 400 ms. Marginally effects were seen for the words-same conditions in left TPO (ROI 3) and in cuneus/precuneus (ROI 4).

Phase-locking

Lastly, we performed phase-locking analyses for picture and words conditions in the time window of 400–700 ms. In Fig. 7, significant phase locking values (PLVs; p < .01) between selected sensor pairs are represented as solid lines on top of topographical maps (see Data analysis: phase-locking section for details). For picture conditions, the twelve sensors, which were most sensitive to differences between conditions, encompassed left temporal, right occipital, and right temporal sites. There were 19 significant PLVs during initial picture presentations (first), compared to 8 significant PLVs in response to repeated pictures (same), and 9 significant PLVs in response to pictures that had been preceded by words (different). A χ^2-test revealed that this distribution of significant synchronized sensor pairs was unlikely to be uniform ($\chi^2 = 6.2, p = .045$). For word stimuli, eleven sensors over bilateral temporal regions were found to be most sensitive to differences between conditions. The distribution of significant PLVs (11 vs. 8 vs. 6) did not differ between conditions ($\chi^2 = 1.6, p = .44$).

**Discussion**

The primary objective of the current study was to examine whether induced gamma band suppression effects can be dissociated at perceptual and conceptual levels of visual object processing; i.e., we wanted to
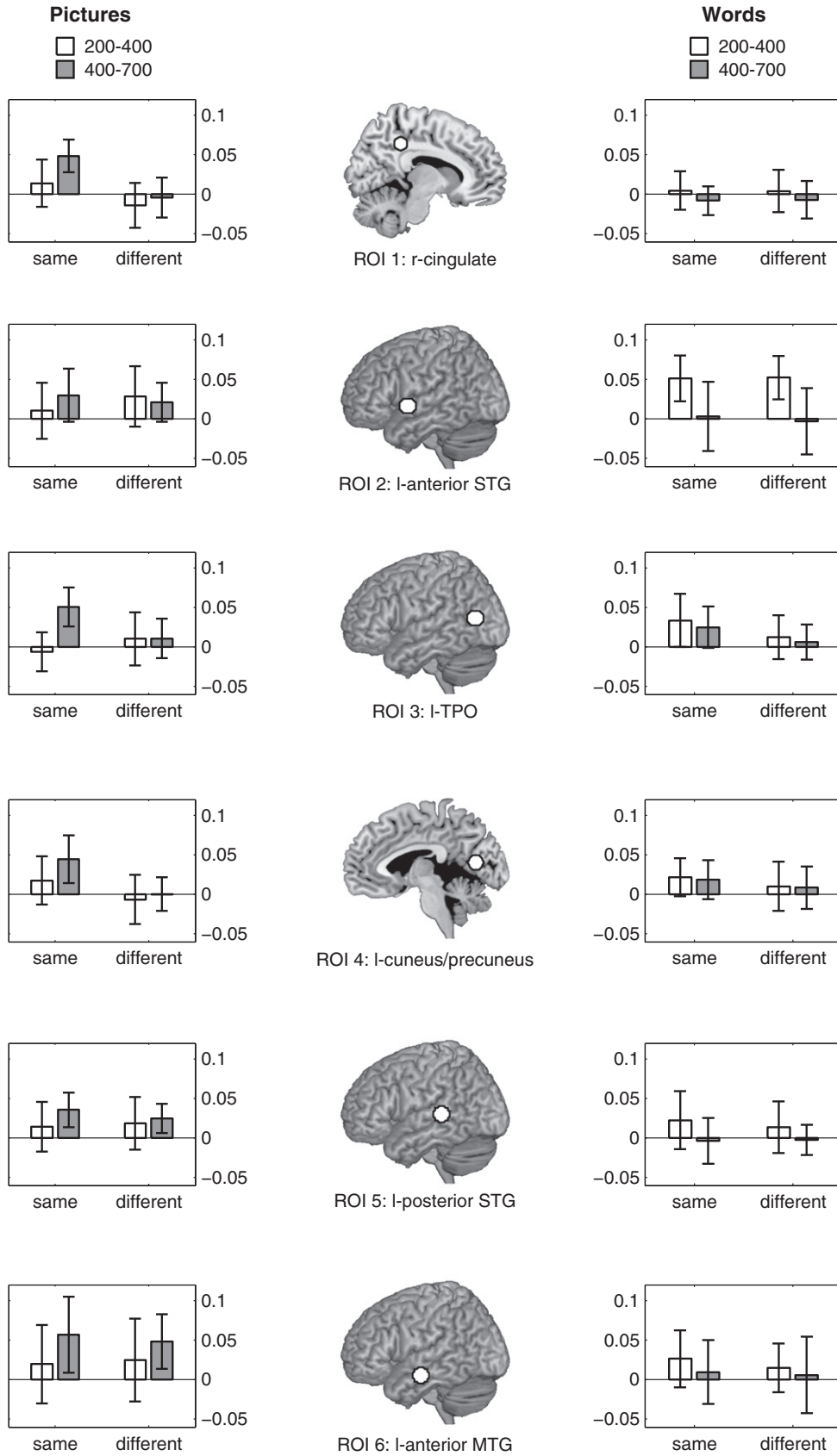
Fig. 6. Induced GBR repetition effects in source space. The middle column depicts the six regions of interest in which iGBA source amplitude changes with respect to baseline for picture and word stimuli in two time windows (200–400 ms and 400–700 ms) were averaged. Bars represent grand mean repetition effects analogous to priming effects. Differences were built between responses to first presentations and repetitions of an object in the identical stimulus domain (same) as well as between first presentations and repetitions of an object in the other stimulus domain (different). Error bars indicate 95% confidence intervals. Asterisks (*) indicate significant priming. (For abbreviations see Fig. 5.)
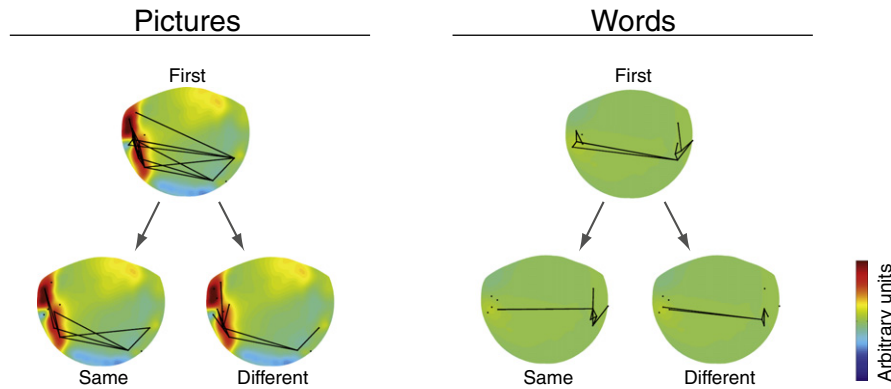
Fig. 7. Phase-locking in the gamma band between selected sensors projected onto spherical spline interpolated topographical maps. Lines indicate significant phase-locking between sensor pairs. The topographical maps were created by averaging the forward solutions (based on the source ROIs) for picture conditions and word conditions respectively. See Methods section for details.

demonstrate iGBA repetition suppression corresponding to repetition priming on the one hand, and conceptual priming on the other hand. Most importantly, we sought to identify brain sources underlying the iGBA reduction showing a regionally distinct and separable tomographic pattern for each processing level. To this aim, we presented repeatedly pictures of real world objects and words denoting the same objects in the context of an implicit memory test (priming). While each participant was confronted with a series of stimuli, pictures could prime subsequent picture or word presentations and, vice versa, words could constitute primes for subsequently presented words or pictures. Volumetric source analysis (VARETA) was carried out in two time windows, 200–400 ms and 400–700 ms. We found a decrease of induced gamma band activity due to repeated presentation of identical pictures in the posterior cingulate cortex 200–400 ms after stimulus onset, and in bilateral occipital cortices and left temporal areas 400–700 ms after stimulus onset. For pictures which had been preceded by their semantically corresponding words, induced gamma band suppression was restricted to the left temporal cortex areas between 400 and 700 ms. In the same time frame, phase synchrony was larger during initial picture processing as compared to subsequently presented pictures, irrespective of the stimulus domain of the prime. Primed words were associated with domain-independent repetition suppression effects in left anterior STG (200–400 ms). Effects in left TPO (400–700 ms) were restricted to same-domain repetitions. Taken together, our findings provide clear support for the notion that repetition-dependent iGBA suppression effects also reflect facilitated conceptual processing in correspondence to conceptual picture priming—complementing previous findings of within-in-domain repetition suppression. For pictures, this conceptual iGBA repetition suppression evolved in left temporal brain regions not until 400–700 ms. For words, conceptual iGBA repetition suppression was observed from 200 to 400 ms also in left temporal cortex.

Recently, it has been argued that scalp EEG-recorded iGBA peaks might be contaminated with ocular artifacts as they coincide with the increased appearance of microsaccades after a display change (Yuval-Greenberg et al., 2008; Keren et al., 2010). We believe our results are not critically affected by this issue for the following reasons. Importantly, here we recorded MEG data, and although in principle MEG recordings might be similarly affected by microsaccade-dependent artifacts, the sensor topographies of iGBA found in our study do not seem to be compatible with ocular sources. For scalp-recorded EEG, it was shown that in dependence of the chosen reference artifactual iGBA reaches maximal amplitudes at central posterior electrodes. For MEG, constituting a reference-free recording technique, any muscular activity originating from around the orbital cavities of the eyes would map to frontal sensors. In fact, any ocular activity-dependent artifacts within the gamma band have to be

revealed by frontal maxima in the MEG sensor topography, which is not the case in our results (see Fig. 3B). Jerbi et al. (2009), using intracerebral EEG-recordings, found saccade-related effects only in the immediate vicinity of the extraocular muscle at the poles of the temporal lobes. In addition, we also analyzed data from a rather late time window (after 400 ms post-stimulus) which should be less prone to the effects of microsaccades. Accordingly, Keren et al. (2010) identified the maximum of artifactual induced gamma power amplitudes approximately 250 ms after stimulus onset with a recovery to baseline after approximately 500 ms.

A possible limitation of our study is that the iGBA results might reflect preparation, and to some degree, execution of motor responses. This possibility cannot be ruled out completely given our choice of the experimental paradigm. However, if iGBA suppression effects were merely driven by activity related to motor responses, the pattern of modulated iGBA sources for picture and word conditions should be comparable—which is clearly not the case. Moreover, there is evidence that fast motor responses are rather associated with strong occipital iGBA, and slow responses relate to weaker iGBA (Hoogenboom et al., 2010). Thus, in our study, this effect would counteract the iGBA suppression which we found to accompany faster behavioral responses. For these reasons we are confident that iGBA suppression effects in this study rather relate to the activation and manipulation of cortical object representations.

Related electrophysiological evidence

Several lines of research provide converging evidence for the notion that iGBA reflects the activation and processing of cortical object representations beyond lower perceptual levels. One set of studies utilized experimental paradigms targeting iGBA changes dependent on crossmodal coherence of the stimulus material (Schneider et al., 2008; Schneider et al., 2011). For objects presented in coherent visual and auditory modalities (e.g., a picture of an animal paired with the sound produced by that animal) increased iGBA was found compared to conditions with incongruent picture-sound pairings (Schneider et al., 2008). Hence, iGBA changes seem to occur at least at the level of multisensory integration. In another series of EEG experiments, it has been established that iGBA suppression can be observed for repeatedly presented familiar object pictures, and iGBA power increases occur for repeatedly presented unfamiliar object pictures (e.g., Gruber and Müller, 2005; Gruber and Müller, 2006; Conrad et al., 2007). These studies have also revealed a corresponding pattern with respect to phase synchrony which was found to decrease for repeated meaningful object and to increase for meaningless objects. This is relevant because phase-locking between pairs of electrodes has been argued to be a more

specific indicator of long-range synchrony between cortical regions (Rodriguez et al., 1999). Importantly, Gruber et al. (2008) replicated these iGBA power and phase synchrony effects in an MEG study. In line with these results, iGBA suppression was found for repeated words but not for repeated pseudowords (Fiebach et al., 2005), and no suppression occurred for abstract contour shapes (Busch et al., 2008). This pattern of results converges on the proposal that neural suppression reflects the sharpening of neuronal representation networks (Henson et al., 2000), whereas increased iGBA rather represents the formation of such networks (Gruber and Müller, 2005).

Our early time interval 200–400 ms corresponds roughly to the typically examined time windows around 160–440 ms after stimulus onset (Gruber and Müller, 2005; Fiebach et al., 2005; Gruber and Müller, 2006; Gruber et al., 2006a; Conrad et al., 2007; Gruber et al., 2008). Note however, that iGBA in these EEG studies might be contaminated by miniature eye movement artifacts to some degree. Nevertheless, consistent with the bilateral posterior topographies reported in these previous studies, we localized the source of this early iGBA domain-specific suppression in the posterior cingulate cortex. In the later interval 400–700 ms, repetition suppression was dissociated for domain-specific and cross-domain effects in parietal–occipital and temporal regions respectively. The iGBA suppression for pictures which were primed by their semantically corresponding words in our study provides strong support for a semantic nature of iGBA effects. Concerning the underlying generators of the scalp-recorded activity, Gruber et al. (2006b) identified a network of temporal, parietal, and occipital regions during familiar and unfamiliar object recognition. Due to the use of undirected statistical tests, that study was not suited to discriminate functional roles of regions within the network of sources underlying the iGBA differences between familiar and unfamiliar objects. On the basis of our results, we are now able to specify the proposed network in more detail. Induced GBA suppression effects in posterior cingulate (200–400 ms) and bilateral parieto-occipital (400–700 ms) areas seem to reflect primarily stimulus-specific processing. These regions were associated with iGBA decrease in response to repeated picture processing (pictures-same). Suppression effects in the left temporal cortex after 400–700 ms appear to be driven in particular by conceptual object features, represented as the only cortical areas residing a significant iGBA decline for conceptually primed pictures (pictures-different). Notably, the left temporal cortex was also the area associated with crossmodal semantic matching processes by Schneider et al. (2008) using a different source modeling approach (linear beamformer estimates; Gross et al., 2001). Thus, there is converging evidence that iGBA reflects access and manipulation of higher-level representations in this brain area.

Interestingly, the results pattern for primed words was quite different. Conceptual iGBA suppression effects for words primed by pictures were seen in left anterior STG (200–400 ms). Same-domain repetition suppression was evident in left anterior STG (200–400 ms) and in the left TPO area (400–700 ms). Numerous evidence exist that both of these regions are involved in lexical processing (Binder et al., 2003; Binder et al., 2009). Our finding of differential timing and localization of conceptual iGBA repetition suppression for the two stimulus domains most likely reflects the distinct processing requirements for pictures and words under the task used. More research is clearly necessary to specify the precise processes involved in conceptual priming since even from behavioral studies it is still controversial under which conditions cross-domain priming of words can be expected. One important precondition is the existence of a conceptual task (Martens and Kiefer, 2009; Kiefer and Martens, 2010), but even then, cross-domain priming is not found consistently (Vriezen et al., 1995; Bowers and Turner, 2003).

Although our analysis of oscillatory brain activity covered nearly the whole range of frequency bands, our results revealed significant conceptual suppression effects exclusively in the induced gamma band. There was some indication for modulation of induced alpha

band activity for same-domain repetitions in sensor space. For instance, over left temporal sensors, alpha band power reductions decreased for repeated-same stimuli which might indicate reduced processing demands. However, these sensor space alpha band effects were not associated with significant results in source space, and given our main interest in iGBA suppression we did not further explore these effects.

To sum up, our results suggest that source iGBA analyses allow to identify the processing of different components of cortical object representations (perceptual vs. conceptual) in space and time. In contrast, most previous EEG/MEG studies on iGBA suppression effects (a) employed repeated presentations of identical stimuli only, (b) analyses of repetition effects have mostly been limited to the peak amplitude of the iGBA, and (c) few studies localized the effects in source space. Notably, the involvement of temporal cortex regions in conceptual priming has not been demonstrated using estimates of iGBA.

Related fMRI/PET findings

Functional magnetic resonance imaging (fMRI) and positron emission tomography (PET) neuroimaging studies have generated abundant evidence for repetition-dependent modulations in a network of areas in frontal, temporal, parietal, and occipital cortices (Henson, 2003; Schacter et al., 2007). For instance, the repeated presentation of pictures was accompanied by decline of BOLD (blood oxygenation level dependent) signals in lateral occipital and inferior frontal areas (Koutstaal et al., 2001). In a recent fMRI study, picture primes induced repetition suppression for word targets in a fronto-temporo-parietal network (Kircher et al., 2009). Similar networks were identified for unimodal word prime and target stimuli by Fiebach et al. (2005) using fMRI and EEG measurements, as well as by Dale et al. (2000) based on fMRI and MEG. Overall, regions in the occipito-temporal cortices have been consistently found to be implicated in various aspects of conceptual processing (Martin and Chao, 2001; Damasio et al., 2004; Binder et al., 2009). In particular, a progression from primarily visual and perceptual feature processing in posterior occipito-temporal regions, to higher-level semantic processing in more anterior regions has been proposed (e.g., Martin and Chao, 2001; Simons et al., 2003). Our results concerning same-domain and cross-domain effects are in good agreement with this functional segregation of occipital and temporal areas, and with the proposal that neural sharpening is reflected by repetition suppression (Desimone, 1996; Wiggs and Martin, 1998). We assume, iGBA reflects (re-) activation and modulation of cortical object representations comprising both low-level perceptual and high-level conceptual features. Depending on the task, the time course and the regional distribution of iGBA could reflect various processes operating on components of these representations. Osipova et al. (2006), e.g., suggested that sustained iGBA might reflect processes by which a cortical object representation is maintained or reinforced—possibly by top-down influence of regions involved in working memory operations. Of course, given our data, this is only speculation, and the precise time course and interplay of brain regions involved demands further research.

Conclusions

This MEG study of human induced gamma band activity (60–90 Hz) provides evidence for repetition-dependent suppression effects that can be modulated at the perceptual as well as at the conceptual level. Left temporal cortex regions were associated with conceptual, cross-domain repetition suppression effects. In contrast, the suppression effects triggered by same-domain repetitions were observed in more posterior regions in and at the boundary of the occipital cortex. This pattern of results suggests that MEG recorded induced gamma band activity in left temporal areas represents the neuronal signatures of conceptual representations, whereas activity in

posterior temporal–parietal–occipital areas reflects perceptual aspects of higher-order visual object processing. At a more general level, an important implication of our study is that the analysis of iGBA in source space can be used to tap into the processing of cortical object representations with respect to different levels of representations, and the localization of these processes in the human brain with high temporal and spectral resolution.

Acknowledgments

References

Alario, F.X., Ferrand, L., 1999. A set of 400 pictures standardized for French: norms for name agreement, image agreement, familiarity, visual complexity, image variability, and age of acquisition. Behav Res Methods Instrum Comput 31 (3), 531–552.

Bertrand, O., Pantev, C., 1994. Stimulus frequency dependence of the transient oscillatory auditory evoked response (40 Hz) studied by electric and magnetic recordings in humans. In: Pantev, C., Elbert, T., Lütkenhöner, B. (Eds.), Oscillatory Event-Related Brain Dynamics, pp. 231–242.

Binder, J.R., McKiernan, K.A., Parsons, M.E., Westbury, C.F., Possing, E.T., Kaufman, J.N., et al., 2003. Neural correlates of lexical access during visual word recognition. J Cogn Neurosci 15 (3), 372–393.

Binder, J.R., Desai, R.H., Graves, W.W., Conant, L.L., 2009. Where is the semantic system? A critical review and meta-analysis of 120 functional neuroimaging studies. Cereb Cortex 19 (12), 2767–2796.

Bosch-Bayard, J., Valdes-Sosa, P., Virues-Alba, T., Aubert-Vazquez, E., John, E.R., Harmony, T., et al., 2001. 3D statistical parametric mapping of EEG source spectra by means of variable resolution electromagnetic tomography (VARETA). Clin Electroencephalogr 32 (2), 47–61.

Bowers, J.S., Turner, E.L., 2003. In search of perceptual priming in a semantic classification task. J Exp Psychol Learn Mem Cogn 29 (6), 1248–1255.

Busch, N.A., Groh-Bordin, C., Zimmer, H.D., Herrmann, C.S., 2008. Modes of memory: early electrophysiological markers of repetition suppression and recognition enhancement predict behavioral performance. Psychophysiology 45 (1), 25–35.

Conrad, N., Giabbiconi, C.M., Müller, M.M., Gruber, T., 2007. Neuronal correlates of repetition priming of frequently presented objects: insights from induced gamma band responses. Neuroscience Letters 429 (2–3), 126–130.

Dale, A.M., Liu, A.K., Fischl, B.R., Buckner, R.L., Belliveau, J.W., Lewine, J.D., et al., 2000. Dynamic statistical parametric mapping: combining fMRI and MEG for high-resolution imaging of cortical activity. Neuron 26 (1), 55–67.

Damasio, H., Tranel, D., Grabowski, T., Adolphs, R., Damasio, A., 2004. Neural systems behind word and concept retrieval. Cognition 92 (1–2), 179–229.

Desimone, R., 1996. Neural mechanisms for visual memory and their role in attention. Proceedings of the National Academy of Sciences of the United States of America 93 (24), 13494–13499.

Engel, A.K., Fries, P., Singer, W., 2001. Dynamic predictions: oscillations and synchrony in top-down processing. Nature Reviews. Neuroscience 2 (10), 704–716.

Fiebach, C.J., Gruber, T., Supp, G.G., 2005. Neural mechanisms of repetition priming in occipitotemporal cortex: spatiotemporal evidence from functional magnetic resonance imaging and electroencephalography. Journal of Neuroscience 25 (13), 3414–3422.

Fries, P., Scheeringa, R., Oostenveld, R., 2008. Finding gamma. Neuron 58 (3), 303–305.

Genovese, C.R., Lazar, N.A., Nichols, T., 2002. Thresholding of statistical maps in functional neuroimaging using the false discovery rate. Neuroimage 15 (4), 870–878.

Grill-Spector, K., Henson, R., Martin, A., 2006. Repetition and the brain: neural models of stimulus-specific effects. Trends Cogn Sci 10 (1), 14–23.

Gross, J., Kujala, J., Hamalainen, M., Timmermann, L., Schnitzler, A., Salmelin, R., 2001. Dynamic imaging of coherent sources: studying neural interactions in the human brain. Proceedings of the National Academy of Sciences of the United States of America 98 (2), 694–699.

Gruber, T., Müller, M.M., 2002. Effects of picture repetition on induced gamma band responses, evoked potentials, and phase synchrony in the human EEG. Brain Research 13 (3), 377–392.

Gruber, T., Müller, M.M., 2005. Oscillatory brain activity dissociates between associative stimulus content in a repetition priming task in the human EEG. Cereb Cortex 15 (1), 109–116.

Gruber, T., Müller, M.M., 2006. Oscillatory brain activity in the human EEG during indirect and direct memory tasks. Brain Research 1097 (1), 194–204.

Gruber, T., Giabbiconi, C.M., Trujillo-Barreto, N.J., Müller, M.M., 2006a. Repetition suppression of induced gamma band responses is eliminated by task switching. Eur J Neurosci 24 (9), 2654–2660.

Gruber, T., Trujillo-Barreto, N.J., Giabbiconi, C.M., Valdes-Sosa, P.A., Müller, M.M., 2006b. Brain electrical tomography (BET) analysis of induced gamma band responses during a simple object recognition task. Neuroimage 29 (3), 888–900.

Gruber, T., Maess, B., Trujillo-Barreto, N.J., Müller, M.M., 2008. Sources of synchronized induced gamma-band responses during a simple object recognition task: a replication study in human MEG. Brain Research 1196, 74–84.

Haenschel, C., Bittner, R.A., Waltz, J., Haertling, F., Wibral, M., Singer, W., et al., 2009. Cortical oscillatory activity is critical for working memory as revealed by deficits in early-onset schizophrenia. Journal of Neuroscience 29 (30), 9481–9489.

Hassler, U., Trujillo Barreto, N., Gruber, T., 2011. Induced gamma band responses in human EEG after the control of miniature saccadic artifacts. Neuroimage 57 (4), 1411–1421.

Henson, R.N., 2003. Neuroimaging studies of priming. Progress in Neurobiology 70 (1), 53–81.

Henson, R.N., Rugg, M.D., 2003. Neural response suppression, haemodynamic repetition effects, and behavioural priming. Neuropsychologia 41 (3), 263–270.

Henson, R., Shallice, T., Dolan, R., 2000. Neuroimaging evidence for dissociable forms of repetition priming. Science 287 (5456), 1269–1272.

Hoogenboom, N., Schoffelen, J.M., Oostenveld, R., Fries, P., 2010. Visually induced gamma-band activity predicts speed of change detection in humans. Neuroimage 51 (3), 1162–1167.

Jensen, O., Kaiser, J., Lachaux, J.P., 2007. Human gamma-frequency oscillations associated with attention and memory. Trends in Neurosciences 30 (7), 317–324.

Jerbi, K., Freyermuth, S., Dalal, S., Kahane, P., Bertrand, O., Berthoz, A., et al., 2009. Saccade related gamma-band activity in intracerebral EEG: dissociating neural from ocular muscle activity. Brain Topogr 22 (1), 18–23.

Keren, A.S., Yuval-Greenberg, S., Deouell, L.Y., 2010. Saccadic spike potentials in gamma-band EEG: characterization, detection and suppression. Neuroimage 49 (3), 2248–2263.

Kiefer, M., Martens, U., 2010. Attentional sensitization of unconscious cognition: task sets modulate subsequent masked semantic priming. J Exp Psychol Gen 139 (3), 464–489.

Kircher, T., Sass, K., Sachs, O., Krach, S., 2009. Priming words with pictures: neural correlates of semantic associations in a cross-modal priming task using fMRI. Hum Brain Mapp 30 (12), 4116–4128.

Koutstaal, W., Wagner, A.D., Rotte, M., Maril, A., Buckner, R.L., Schacter, D.L., 2001. Perceptual specificity in visual object priming: functional magnetic resonance imaging evidence for a laterality difference in fusiform cortex. Neuropsychologia 39 (2), 184–199.

Lachaux, J.P., Rodriguez, E., Martinerie, J., Varela, F.J., 1999. Measuring phase synchrony in brain signals. Hum Brain Mapp 8 (4), 194–208.

Loftus, G.R., Masson, M.E.J., 1994. Using confidence intervals in within-subject designs. Psychonomic Bulletin & Review 1 (4), 476–490.

Martens, U., Kiefer, M., 2009. Specifying attentional top-down influences on subsequent unconscious semantic processing. Advances in cognitive psychology 9, 56–68.

Martin, A., Chao, L.L., 2001. Semantic memory and the brain: structure and processes. Current Opinion in Neurobiology 11 (2), 194–201.

Matsumoto, A., Iidaka, T., 2008. Gamma band synchronization and the formation of representations in visual word processing: evidence from repetition and homophone priming. J Cogn Neurosci 20 (11), 2088–2096.

Osipova, D., Takashima, A., Oostenveld, R., Fernandez, G., Maris, E., Jensen, O., 2006. Theta and gamma oscillations predict encoding and retrieval of declarative memory. Journal of Neuroscience 26 (28), 7523–7531.

Race, E.A., Badre, D., Wagner, A.D., 2010. Multiple forms of learning yield temporally distinct electrophysiological repetition effects. Cereb Cortex 20 (7), 1726–1738.

Rodriguez, E., George, N., Lachaux, J.P., Martinerie, J., Renault, B., Varela, F.J., 1999. Perception's shadow: long-distance synchronization of human brain activity. Nature 397 (6718), 430–433.

Schacter, D.L., Wig, G.S., Stevens, W.D., 2007. Reductions in cortical activity during priming. Current Opinion in Neurobiology 17 (2), 171–176.

Schneider, T.R., Debener, S., Oostenveld, R., Engel, A.K., 2008. Enhanced EEG gamma-band activity reflects multisensory semantic matching in visual-to-auditory object priming. Neuroimage 42 (3), 1244–1254.

Schneider, T.R., Lorenz, S., Senkowski, D., Engel, A.K., 2011. Gamma-band activity as a signature for cross-modal priming of auditory object recognition by active haptic exploration. Journal of Neuroscience 31 (7), 2502–2510.

Simons, J.S., Koutstaal, W., Prince, S., Wagner, A.D., Schacter, D.L., 2003. Neural mechanisms of visual object priming: evidence for perceptual and semantic distinctions in fusiform cortex. Neuroimage 19 (3), 613–626.

Snodgrass, J.G., Vanderwart, M., 1980. A standardized set of 260 pictures: norms for name agreement, image agreement, familiarity, and visual complexity. J Exp Psychol Hum Learn 6 (2), 174–215.

Tallon-Baudry, C., Bertrand, O., 1999. Oscillatory gamma activity in humans and its role in object representation. Trends Cogn Sci 3 (4), 151–162.

Tallon-Baudry, C., Bertrand, O., Delpuech, C., Permier, J., 1997. Oscillatory gamma-band (30–70 Hz) activity induced by a visual search task in humans. Journal of Neuroscience 17 (2), 722–734.

Varela, F., Lachaux, J.P., Rodriguez, E., Martinerie, J., 2001. The brainweb: phase synchronization and large-scale integration. Nature Reviews. Neuroscience 2 (4), 229–239.

Voss, J.L., Schendan, H.E., Paller, K.A., 2010. Finding meaning in novel geometric shapes influences electrophysiological correlates of repetition and dissociates perceptual and conceptual priming. NeuroImage 49 (3), 2879–2889.

Vriezen, E.R., Moscovitch, M., Bellos, S.A., 1995. Priming effects in semantic classification tasks. Journal of Experimental Psychology: Learning, Memory, and Cognition, Vol 21 (4), 933–946.

Wagner, A.D., Maril, A., Schacter, D.L., 2000. Interactions between forms of memory: when priming hinders new episodic learning. J Cogn Neurosci 12 (Suppl 2), 52–60.

Wiggs, C.L., Martin, A., 1998. Properties and mechanisms of perceptual priming. Current Opinion in Neurobiology 8 (2), 227–233.

Yuval-Greenberg, S., Tomer, O., Keren, A.S., Nelken, I., Deouell, L.Y., 2008. Transient induced gamma-band response in EEG as a manifestation of miniature saccades. Neuron 58 (3), 429–441.